

Trapping and aligning carbon nanotubes via substrate geometry engineering

Y M Wang, Wei-Qiang Han and A Zettl

Department of Physics, University of California at Berkeley, and
Materials Sciences Division, Lawrence Berkeley National Laboratory,
Berkeley, CA 94720, USA
E-mail: azettl@socrates.berkeley.edu

New Journal of Physics **6** (2004) 15

Received 7 October 2003

Published 4 February 2004

Online at <http://www.njp.org/> (DOI: 10.1088/1367-2630/6/1/015)

Abstract. We present a simple method to place pregrown carbon nanotubes at specified locations on geometrically patterned silicon devices. Following room-temperature solution deposition, the nanotubes span gaps between pairs of tooth-shaped anchors serving as mechanical and/or electrical contacts. With a single deposition step, at least 50% of the anchor pairs are spanned by nanotubes. With the simultaneous application of modest local electric fields during deposition, the yield of successfully spanned anchor pairs is increased to 100%. Our placement method may find application in the reliable fabrication of nanotube-based electronic and microelectromechanical systems (MEMS) devices.

The unique electronic and mechanical properties of carbon nanotubes (CNTs) make these systems attractive for incorporation into next-generation electronic and microelectromechanical systems (MEMS) devices. Indeed, many prototype CNT-based devices have already been demonstrated, including room-temperature rectifiers [1], field-effect transistors [2, 3], random-access-memory devices [4], electron field emitters [5, 6], sensitive gas detectors [7, 8] and nanoscale rotational actuators and motors [9].

In addition to radical architectures which exploit random configurations of nanotubes [4], the placement of individual nanotubes or nanotube bundles with respect to other device substructures is critical. In some test devices, selected nanotubes have been located individually by laborious scanned-probe techniques including scanning-tunnelling microscopy [1] and atomic-force microscopy [10], where the microscope tip also serves as the measurement probe (of electronic and/or mechanical response). Alternatively, nanotubes have been deposited on substrates and their position subsequently identified via suitable microscopies, followed by a 'wiring up' of the nanotubes using electrical contacts defined by electron-beam lithography [2, 3].

Unfortunately, such ‘individual nanotube’ manipulation or selection methods do not lend themselves well to commercial mass-produced products, and alternative techniques employing directed growth or directed deposition of nanotubes are needed. Efforts at controlling CNT placement have followed basically two approaches: synthesizing CNTs directly at high temperature from patterned catalysts using chemical vapour deposition [11, 12] or depositing solution-suspended CNTs using pretreated (i.e. chemically functionalized) substrates [13]–[17]. Neither approach has complete control of the location, orientation, and quantity of the deposited nanotubes.

We here describe a room-temperature method whereby pregrown carbon nanotubes can be deposited from solution at specified locations on a clean geometrically patterned silicon device. Following the deposition, the nanotubes typically span pairs of tooth-shaped anchors serving as mechanical and/or electrical contacts. The effectiveness of the placement is enhanced by the application of local electric fields during the deposition.

Multi-wall and single-wall carbon nanotubes used for this study have been synthesized locally using a pyrolysis method [18] or obtained commercially (Carbon Nanomaterials, Inc.). Tube lengths range from a few μm to over $100\ \mu\text{m}$. The purified nanotubes are suspended in acetone by sonication for 15 min and deposited via a glass pipette directly onto the recipient device. The pre-patterned MEMS-type substrate test devices are typically created using silicon-on-insulator (SOI) wafers. Following conventional lithographic patterning, the Si overlayer is selectively etched all the way through releasing the $50\text{-}\mu\text{m}$ -thick Si test device from the underlying support structure.

Figure 1(a) shows (using scanning electron microscope (SEM) imaging) an example of a trench device incorporating many opposing tooth-shaped anchors. The large, crescent-shaped depressions on the left and right of the device are fluid reservoirs. The concentric rings closer to the centre are troughs that cut all the way through the device and serve to control fluid motion during the fluid-drying stage (described below). The transverse cut through these rings, which in figure 1(a) is oriented from the upper left to lower right of the figure, is where the anchor teeth are located. All along this diagonal cut, the opposing trench walls are serrated with uniformly patterned teeth. The inset to figure 1 shows a magnified view of the opposing teeth, which are slightly offset so as to localize the region of closest approach. The closest approach regions are the locations where nanotube placement is desired, i.e. the goal is to span nanotubes across the smallest gap between opposing teeth.

To accomplish the nanotube placement on the device, the device is suspended horizontally in air with forceps and a droplet of the nanotube-containing acetone is placed on top of the device. The droplet bulges out on both the top and bottom of the device. Within one or two minutes, the droplet dries. Subsequent SEM imaging reveals that both the top and bottom surfaces of the teeth pairs are spanned by either individual CNTs or CNT bundles, depending on the suspension preparation. Figure 1(b) shows a single multiwall nanotube connecting an anchor pair. The nanotube spans straight across without sagging. The device area in the vicinity is clean and free of nanotubes. The ratio of the number of tooth pairs connected by one or a few nanotubes to the total number of pairs on the device is defined as the successful deposition rate. For this simple ‘fluid drying’ deposition method, the successful deposition rate is approximately 50%. We have experimented with different tooth patterns such as triangular pairs and other pointed pairs, and found lower deposition rates (approximately 20%). Within our trial device configuration shown in figure 1, the mismatched rectangular tooth apparently provides the optimal geometry.

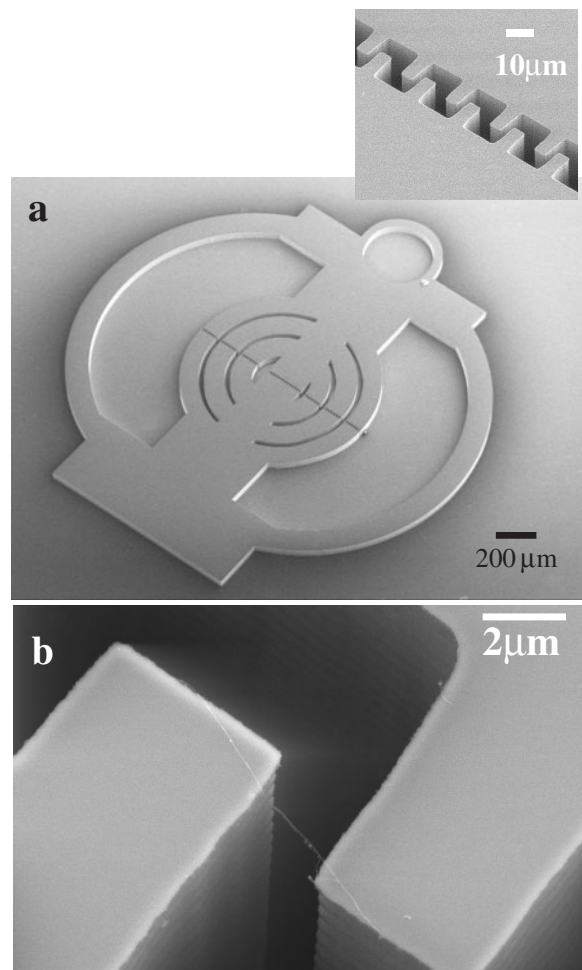


Figure 1. (a) Scanning electron microscope image of the silicon MEMS device for CNT depositions. The inset shows the tooth pairs in the centre of the device. (b) A straight CNT stretches across a pair of contacts. Note that the area in the vicinity is clean.

What mechanism attracts the suspended CNTs towards the tooth pairs? We believe it is a combination of strong capillary force generated by the narrow centre trench, surface-tension effects which drag nanotubes along as the droplet dries and the strong interaction of nanotubes with clean silicon surfaces. The width of the serrated trench in the device of figure 1 ranges from $2\ \mu\text{m}$ at regions in between a tooth pair to more than $10\ \mu\text{m}$ between pairs. Micrometre-sized gaps are narrow enough for capillary forces to become important. When a droplet is deposited, the acetone is attracted to the trench from all directions. Since capillary pressure is inversely proportional to the size of an opening, the strongest force is located between a pair of teeth. Here a nanotube makes good contact with the Si edges and stays intact for the rest of the drying process. Lesser bonded tubes are swept away as the droplet/air interface front passes through.

To help confirm the role played by capillary action and to optimize the device geometries, we have found it instructive to observe directly with an optical microscope the acetone drying process for devices of different geometry. For example, for the device of figure 1, the depressed

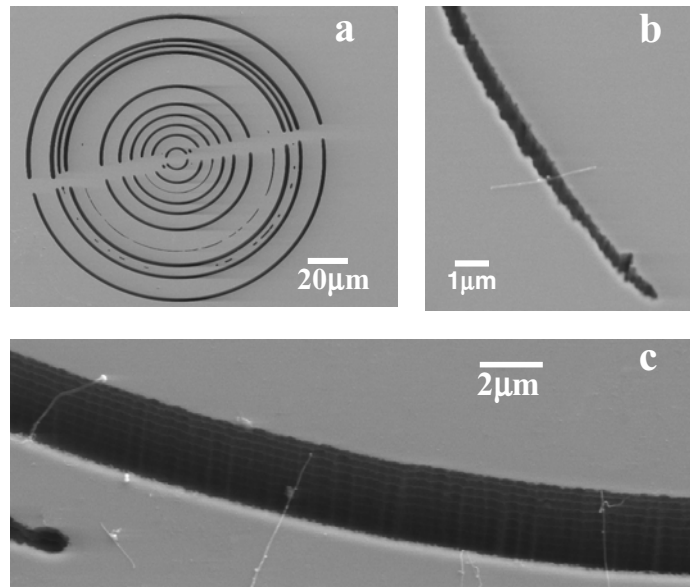


Figure 2. (a) Circular trenches in the centre of the device. (b) A single nanotube and (c) three parallel nanotubes stretch across the trenches. Some short nanotubes land nearby in (c), since they are not long enough to span the gap.

areas of the device dry first and acetone retreats to the centre and the outer ring of the device. In the centre, acetone dries first distant from the serrated cut, taking the unconnected nanotubes with it and forms droplets in the upper and lower parts of the device (subsequent SEM imaging shows nanotubes only at the upper and lower centres of the device and few elsewhere). Finally, the centre trench, up to now always filled with acetone, starts to dry. The capillary force draws nearby acetone with suspended nanotubes into the trench until all fluid has evaporated.

The 50% yield refers to a single deposition step. One might expect this to increase if subsequent depositions are performed on the same device, and indeed this is the case. However, using this procedure, the deposition rate never reaches 100%. For unknown reasons (perhaps local contamination), some tooth pairs are adverse to trapping nanotubes using the ambient drying method alone, no matter how many droplets are sequentially added and allowed to dry (below we describe a slight modification that reliably increases the deposition rate to 100%).

The overall design of the device is important for successful depositions. For example, to help better align the nanotubes, the rings in the centre of the device in figure 1 match the circular symmetry of the whole device. The rings are separated to hasten the acetone drying process. The trench cuts all the way across the device's central region, acting as an open channel for acetone to flow in and out. For trenches that are not etched all the way across, the deposition rate can be as low as 10%.

Alternative geometries that do not employ opposing teeth can also trap and align nanotubes, though not as effectively. Figure 2(a) shows a tooth-free concentric-rings-geometry. For the same deposition method described above, nanotubes align perpendicularly across the trenches. Figures 2(b) and (c) show a single and three parallel CNTs spanning the trenches, respectively. In figure 2(b), the trench width is intentionally tapered to determine the minimal trench width for effective nanotube trapping. We find a gap cutoff of approximately $1 \mu\text{m}$.

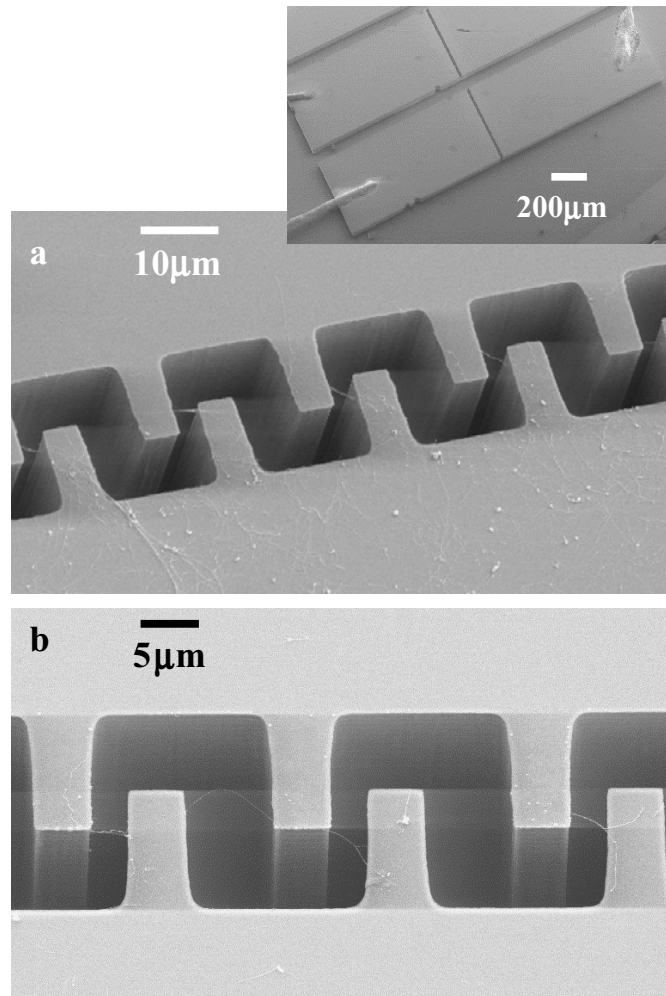


Figure 3. Depositions using electric fields. (a) At a voltage of 6 V, all tooth pairs are connected by single or a few nanotubes. Excess nanotubes land on the anode side of the trench. The cathode remains empty. The inset shows the silicon device used for the deposition. (b) At a higher voltage of 8 V and a lower nanotube concentration, tooth pairs are connected by single CNTs.

van der Waals forces alone apparently trap only a fraction of the nanotubes swept past the tooth pairs. We find that the simultaneous application of local electric fields allows virtually all nanotubes to be trapped. Although electric fields have been used previously in aligning suspended CNTs [12]–[16], individual nanotubes have not been isolated from the aligned nanotube bundles to form functional devices. We custom-designed the chip so that the electric field and the electric-field gradient work together, via dielectrophoresis, to trap and align virtually all nanotubes in a droplet to form single-nanotube-based devices. Nanotubes (semiconducting and metallic) can be considered as point dipoles when polarized in electric fields [19]. The electric field's force on a dipole moment P is $F = \nabla(P \cdot E)$. Since $P \propto E$ for dielectric particles with a linear response, $F \propto \nabla(E \cdot E)$.

A Si device for depositions employing dielectrophoresis is shown in the inset to figure 3(a). The structure consists of two doped Si islands separated by an array of teeth pairs. DC voltages

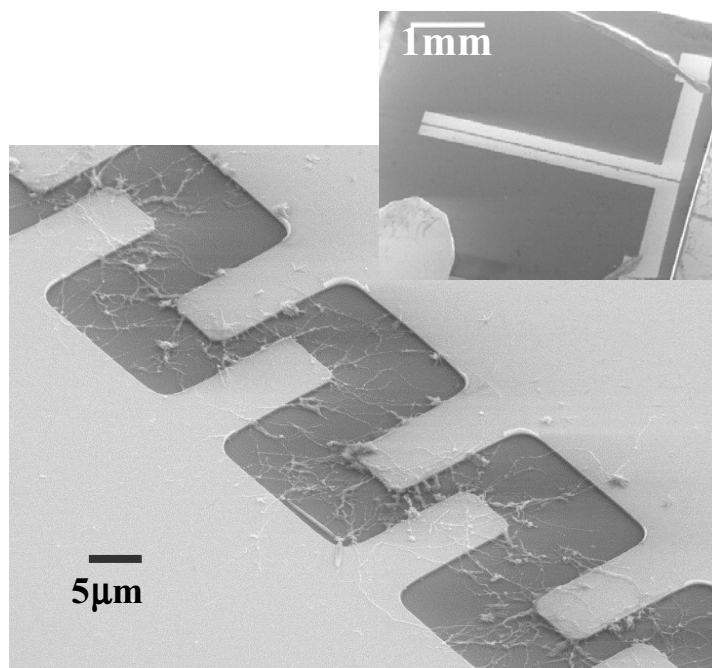


Figure 4. Trapping CNTs using gold electrodes. The inset shows that the gold electrodes occupy only the centre region of the chip. At 10 V, all the nanotubes in the droplet are trapped within the centre gap in alignment with the electric field lines.

are applied across the central trench. In a cylindrical co-ordinate system with the z -axis along the trench direction, the electric field is inversely proportional to the azimuthal distance r as $E \propto 1/r$. The nanotubes can be treated as point dipoles that are always aligned with the electric field. The force $F \propto \nabla(E \cdot E)$ on a nanotube anywhere on the chip points towards the central trench. When the nanotube arrives at the trench, it strongly binds to the tooth pair contacts.

We observe, via optical microscopy, nanotube-rich material rapidly moving towards the trench when an electric field is applied. Figure 3(a) shows the aligned nanotubes deposited with an applied voltage of 6 V. All tooth pairs are connected by one or a few CNTs. Excess nanotubes land on the anode side of the trench. A few nanotubes (<5%) are observed outside the central region. Using a higher voltage and a more dilute nanotube solution, we are able to deposit single nanotubes only. In the device of figure 3(b), single nanotubes aligned at 8 V span all tooth pairs, with no nanotubes observed anywhere else on the chip device.

Without strong capillary forces, can electric fields alone be effective in trapping nanotubes? To answer this question, we studied shallow gold tooth patterns residing on oxide surfaces. The inset to figure 4 shows such a tailored device, where two parallel horizontal bars are separated by a small gap. The gap region, shown in the main body of figure 4, consists of offset opposing gold teeth. With 10 V applied between the teeth during acetone deposition, all nanotubes in the droplet are apparently trapped within the gap along the electric field line directions. No nanotubes are observed outside the gap region. Control experiments without applied electric fields verified the effectiveness of electric field in this geometry. As is evident from figure 4, this is a form of radical and indiscriminant trapping, and even some nanoscale carbon debris is trapped along with the nanotubes. Although useful, we consider this wide gap, electric-field-only method less discriminating in the placement of individual nanotubes at specified locations.

In conclusion, we have demonstrated that, using unique substrate geometries and solution depositions, we are able to trap and align CNTs with a high degree of control. This room-temperature technique should be useful in the development of CNT-based electronic devices.

Acknowledgments

This research was supported by the Director, Office of Energy Research, Office of Basic Energy Sciences, Materials Sciences Division of the US Department of Energy under Contract no. DE-AC03-76SF00098.

References

- [1] Collins P G, Zettl A, Bando H, Thess A and Smalley R E 1997 *Science* **278** 100
- [2] Tans S J, Verschueren A R M and Dekker C 1998 *Nature* **393** 49
- [3] Bockrath M, Hone J, Zettl A, McEuen P L, Rinzler A G and Smalley R E 2000 *Phys. Rev. B* **61** R10606
- [4] Cohen M L, Louie S G and Zettl A 2000 *Solid State Commun.* **113** 549
- [5] de Heer W A, Chatelain A and Ugrate D 1995 *Science* **270** 1179
- [6] Collins P G and Zettl A 1996 *Appl. Phys. Lett.* **69** 1969
- [7] Collins P G, Bradley K, Ishigami M and Zettl A 2000 *Science* **287** 1801
- [8] Franklin J K N, Chou C, Pan S, Cho K J and Dai H 2000 *Science* **287** 622
- [9] Fennimore A M, Yuzvinsky T D, Han W-Q, Fuhrer M S, Cumings J and Zettl A 2003 *Nature* **424** 408
- [10] Falvo M, Taylor II R M, Helser A, Chi V, Brooks Jr F P, Washburn S and Superfine R 1999 *Nature* **357** 236
- [11] Kong J, Soh H T, Cassell A M, Quate C F and Dai H 1998 *Nature* **395** 878
- [12] Zhang Y *et al* 2001 *Appl. Phys. Lett.* **79** 3115
- [13] Yamamoto K, Akita S and Nakayama Y 1996 *Japan. J. Appl. Phys.* **35** L917
- [14] Yamamoto K, Akita S and Nakayama Y 1998 *J. Phys. D: Appl. Phys.* **31** L34
- [15] Chen X Q, Saito T, Yamada H and Matsushige K 2001 *Appl. Phys. Lett.* **78** 3714
- [16] Nagahara L A, Amlani I, Lewenstein J and Tsui R K 2002 *Appl. Phys. Lett.* **80** 3826
Liu J, Casavant M J, Cox M, Walters D A, Boul P, Lu W, Rimberg A J, Smith K A, Colbert D T and Smalley R E 1999 *Chem. Phys. Lett.* **303** 125
- [17] Lewenstein J C, Burgin T P, Ribayrol A, Nagahara L A and Tsui R K 2002 *Nano. Lett.* **2** 443
- [18] Rao C N R, Sen R, Satishkumar B C and Govindaraj J 1998 *J. Chem. Soc. Chem. Commun.* **15** 1525
- [19] Fishbine B H 1996 *Full. Sci. Technol.* **4** 87